Description of collective states in ^{192}Os within the boson expansion theory

H. Sakamoto [*]

Faculty of Engineering, Gifu University, Gifu 501-1193, Japan

The low-lying collective states in ^{192}Os are investigated microscopically by means of the boson expansion theory with the self-consistent effective interactions. The building blocks of the collective boson, the collective potential, and the structures of the wave functions for some relevant states are illustrated. Calculated level energies and electromagnetic properties are compared with the experimental data. Properties of some low-lying states and relevant quasibands are discussed with the help of the boson description of state vectors.

I. INTRODUCTION

Neutron-rich nuclei with mass number $A \approx 190$ provide a characteristic testing ground for microscopic theories of nuclear structures [1–10]. There are quite a few indications that a prolate-oblate shape transition takes place near neutron number $N = 116$ in this mass region [3,6,9–12]. It has been indicated that the lowest $K^{\pi} = 2^{+}$ bands exist in osmium nuclei [13,14] and these nuclei also have low-lying $K^{\pi} = 4^{+}$ bands at about twice the excitation energy of the $K^{\pi} = 2^{+}$ bands, making them good candidates for being a member of a two-phonon doublet [15]. There have been robust discussions on the two-phonon γ-vibrational strength in the osmium nuclei [7,13–20].

The microscopic description of anharmonicities in nuclear quadrupole collective motions, in terms of the fermion degrees of freedom, is a long-standing and fundamental subject in the study of nuclear many-body systems. The boson expansion theory (BET) is a promising method for the subject if the coupling to noncollective states is faithfully included in the calculation [21,22]. It allows us to take into account higher order terms neglected in the random phase approximation (RPA), and the adiabatic condition for particle motions can be avoided.

Earlier applications of the BET to nuclear many-body problems were studied by Sørensen [23] and Lie and Holzwarth [24], and extensive applications of the BET to realistic nuclei, along the lines of practical prescriptions developed by Kishimoto and Tamura [4,5] (referred to as KT-1 and KT-2 below), were worked out by Tamura and his coworkers [6,25–27]. As for the study of the osmium nuclei in terms of the BET, some results were reported in Refs. [6,27] where the formalism of KT-1 and KT-2 were applied to the Hamiltonian of the pairing-plus-quadrupole (P+Q) model of nuclear interactions [28–31] improved by including additionally the quadrupole-pairing interaction.

It was pointed out later, however, that the construction of the formalism of Refs. [4,5] lacked the proof that the KT-2 operators were allowed to act upon the ideal-boson states. Then, the earlier formalism of the BET of KT-1 and KT-2 has been reformulated in a entirely new and mathematically rigorous form as a normal-ordered linked-cluster expansion of the modified Marumori boson mapping [21] (referred to as KT-3).

Applications of the KT-3 formalism to realistic nuclei have been reported in Refs. [32–38]. Regarding the change in the nuclear structure due to the change in the number of neutrons near $N = 116$ in osmium isotopes, calculations by means of the BET along the lines of KT-3 have been briefly reported in Ref. [38]. For the ^{192}Os nucleus, some results of applications of the KT-3 formalism have been reported in Refs. [33,38], but the structures of the wave functions and electromagnetic properties, among others, have not been described in detail except for a brief report in Ref. [38]. It is the purpose of this paper to present and discuss results of further analyses of ^{192}Os, which is of particular interest as a nucleus with $N = 116$, where the γ softness is expected to increase significantly [3,8–11,38–40].

In this paper, the low-lying collective states in ^{192}Os nucleus are investigated microscopically by means of the BET with the self-consistent effective interactions [41,42], which are considered to be advanced interactions following the spirit of the P+Q model of nuclear interactions [28–31]. The KT-3 formalism [21] is applied to construct a microscopic boson image of the fermion Hamiltonian and that of the $E2$ operator. The potential energy surfaces and the structures of boson wave functions for some relevant low-lying collective states are illustrated. Theoretical level energies and electromagnetic properties are compared with the experimental data. Properties of the ground-state band, the quasi-γ band, the 0_2^+ band and the excited 0^+ states, and the $K^{\pi} = 4^+$ band are discussed with the help of the boson description of state vectors.

II. THEORETICAL FRAMEWORK

The theoretical framework is discussed in detail in Refs. [34,35]; here it is described only briefly.

_____
[*]sakamoto@gifu-u.ac.jp

A. Fermion description

The model Hamiltonian adopted in this paper is given in fermion operators as

$$H = h_{\text{s.p.}} + (H_{\text{0-pair}} - \lambda \hat{N}) + H_{\text{2-pair}} + V^{(2)} + V^{(3)} + V^{(4)}, \tag{1}$$

with

$$H_{\text{0-pair}} = -\frac{G_0}{4} \hat{P}_0^\dagger \hat{P}_0, \quad H_{\text{2-pair}} = -\frac{G_2}{2} (\hat{P}_2^\dagger \cdot \hat{P}_2), \tag{2}$$

$$V^{(2)} = -\frac{\chi^{(2)}}{2} (\hat{Q}_2 \cdot \hat{Q}_2), \tag{3}$$

$$V^{(3)} = -\frac{\chi^{(3)}}{3!} [\sqrt{56\pi/5}(\hat{Q}_2 \hat{Q}_2 \hat{Q}_2) - 3\hat{R}_0 (\hat{Q}_2 \cdot \hat{Q}_2)], \tag{4}$$

$$V^{(4)} = -\frac{\chi^{(4)}}{4!} \left[\frac{48\pi}{5} (\hat{Q}_2 \cdot \hat{Q}_2)^2 - 8\sqrt{56\pi/5} \hat{R}_0 (\hat{Q}_2 \hat{Q}_2 \hat{Q}_2) \right.$$
$$\left. + 12\hat{R}_0^2 (\hat{Q}_2 \cdot \hat{Q}_2) \right]. \tag{5}$$

Here $h_{\text{s.p.}}$ is the spherical limit of the Nilsson Hamiltonian [43], and the fermion model space is spanned by $3s_{1/2}$, $2d_{3/2}$, $2d_{5/2}$, $1g_{7/2}$, $2f_{7/2}$, $1h_{9/2}$, $1h_{11/2}$, and $1i_{13/2}$ orbits for protons and $3p_{1/2}$, $3p_{3/2}$, $2f_{5/2}$, $2f_{7/2}$, $1h_{9/2}$, $2g_{9/2}$, $1i_{11/2}$, $1i_{13/2}$, and $1j_{15/2}$ orbits for neutrons. The residual interactions in the fermion Hamiltonian are the monopole- and quadrupole-pairing interactions, $H_{\text{0-pair}}$ and $H_{\text{2-pair}}$, the quadrupole-quadrupole (QQ) interaction, $V^{(2)}$, and the effective three- and four-body interactions, $V^{(3)}$ and $V^{(4)}$. The effective many-body interactions have been introduced as the higher order terms of the QQ interaction to recover the saturation and the self-consistency between the density and the potential in higher order accuracy (*nuclear self-consistency*) [41,42,44–49].

Strengths of the monopole-pairing interactions, $G_0(p)$ for protons and $G_0(n)$ for neutrons, are determined to fit the gap energies through the BCS gap equation. The adopted strengths in the present calculations are $G_0(p) = 27.24/A$ MeV for protons and $G_0(n) = 21.30/A$ MeV for neutrons. These strengths are nearly compatible with the systematics proposed by Copnell *et al.* [50].

The strengths of the quadrupole-pairing interactions are parameterized as $g_2'(p) = G_2(p)/G_2^{\text{self}}(p)$, $g_2'(n) = G_2(n)/G_2^{\text{self}}(n)$, where $G_2^{\text{self}}(p)$ for protons and $G_2^{\text{self}}(n)$ for neutrons are the self-consistent strengths of the quadrupole-pairing interaction to recover the *local Galilean invariance* in the RPA order, respectively [51]. The strengths of the QQ interaction and its higher order terms, $\chi^{(2)}$, $\chi^{(3)}$, and $\chi^{(4)}$, are parametrized as $f_2 = \chi^{(2)}/\chi_2^{\text{self}}$, $f_3 = \chi^{(3)}/\chi_3^{\text{self}}$, $f_4 = \chi^{(4)}/\chi_4^{\text{self}}$, where χ_2^{self}, χ_3^{self}, and χ_4^{self} are the self-consistent values of $\chi^{(2)}$, $\chi^{(3)}$, and $\chi^{(4)}$, respectively, which are derived in Ref. [41]. In the present analyses, to reduce the number of free parameters, these parameters are set to $f_2 = f_3 = f_4 = f$ and $g_2'(p) = g_2'(n) = g'$, and in calculating the energy spectra the two dimensionless parameters, f and g', are varied slightly around the vicinity of the predicted value, i.e., unity. The adopted strengths in the present calculations are $f = 1.15$ and $g' = 1.05$. For comparison, it is estimated for the QQ interaction that the RPA critical strength is $f_2^{\text{RPA}}(\text{crit}) = 0.954$

while the strength to fit the experimental 2_1^+ energy within the RPA is $f_2^{\text{RPA}}(2_1^+) = 0.949$.

In calculating the electromagnetic properties, the $E2$ polarization charge, $e_{\text{pol}}(E2)$, is introduced as the only additional parameter to fit the experimental data. In this work, for simplicity, a common value of $e_{\text{pol}}(E2) = 0.5e$ is adopted for both protons and neutrons. The need for the polarization charge in the present type of analyses, in connection with the choice of the single-particle model space and the omission of the $\Delta N_{\text{osc}} = 2$ quadrupole matrix elements under the presence of the pairing interactions, has been discussed in detail in Refs. [5,35,44]

B. Boson description

In the modified Marumori boson mapping [21,32], orthonormal n boson states, which span the ideal boson space, are introduced as

$$|n : a) \equiv N(n : a)^{-1} A_{a_1}^\dagger A_{a_2}^\dagger \ldots A_{a_n}^\dagger |0), \tag{6}$$

where $A^\dagger$'s are the ideal boson operators and $N(n : a)$ is the boson normalization factor with the abbreviated notation $(n : a) \equiv (a_1, a_2, \ldots, a_n)$ with $a_1 \leqslant a_2 \leqslant \cdots \leqslant a_n$. Corresponding n Tamm-Dancoff (TD) fermion-pair states

$$|n : a \gg \equiv N(n : a)^{-1} B_{a_1}^\dagger B_{a_2}^\dagger \ldots B_{a_n}^\dagger |0 > \tag{7}$$

are not generally orthonormal and linearly independent. Here $B^\dagger$'s are the TD fermion-pair operators. The fermion norm matrix is denoted as $\ll n : a|m : b \gg \equiv \delta_{nm}(Z_n^2)_{a;b}$.

In order to construct orthonormalized fermion states, one has to assume that the inverse of Z_n, i.e., Z_n^{-1}, exists. One of the possible ways would be to divide the fermion space $\{|n : a \gg\}$ into two parts, T_F and $(1 - T_F)$, i.e., the T_F space including the components that are retained and $(1 - T_F)$ excluding those. Then the orthonormalized fermion states can be obtained as

$$|n : t > \equiv \sum_{t'} \left(Z_n^{-1} \right)_{t;t'} |n : t' \gg; \tag{8}$$

here and in the following t, t', etc., indicate the components that belong to the T_F space while $\bar{t}, \bar{t}'$, etc., indicate those that belong to the $(1 - T_F)$ space. To derive a physically meaningful boson mapping, the ideal boson space $\{|n : a)\}$ is also divided into two parts, T and $(1 - T)$; i.e., the truncated space T for boson states is introduced as a replica of the T_F space for the fermion states.

The one-to-one correspondence between the fermion state $|n : t >$ and the boson state $|n : t)$ in the truncated space is obtained by using a mapping operator

$$U = \sum_{(n:t)} |n : t) < n : t| \tag{9}$$

as

$$|n : t) = U|n : t >, \quad |n : t >= U^\dagger |n : t). \tag{10}$$

At the same time, a boson image $(O_F)_B$ of a fermion operator O_F is defined by

$$(O_F)_B \equiv U O_F U^\dagger \tag{11}$$

so as to satisfy

$$< m : t|O_F|n : t' >= (m : t|(O_F)_B|n : t') \qquad (12)$$

in the truncated subspace. The operator U transcribes the dynamics of a fermion system into that of a boson system.

The normal-ordered linked-cluster expansion of $(O_F)_B$ is obtained by expressing $|0)(0|$ and $(Z_n)_{t;t'}$ in an expansion form. For example, the boson image of the basic TD fermion-pair operator can be expanded as

$$(B_{t_1}^\dagger)_B = A_{t_1}^\dagger - \frac{1}{4} \sum_{t_2 t_3 t_4} Y(t_1 t_2 t_3 t_4) A_{t_2}^\dagger A_{t_3}^\dagger A_{t_4} + O(\epsilon^2), \qquad (13)$$

where $Y(abcd) = 2(Y_2)_{ad;bc}$ with the matrix Y_n defined by $Z_n = [1_n - Y_n]^{1/2}$. The ϵ denotes the expansion parameter such as $|Y_2|$ and is usually very small if one truncates the system to the collective TD component [21,32]. In the present numerical calculations, all the TD elements with spin $I \leqslant 4$ are regarded as the chosen TD modes, and among them the lowest quadrupole mode is identified as the collective TD mode. The numbers of the basic TD two-quasiparticle modes having spin $I = 0, 1, 2, 3,$ and 4 which can be constructed within the present single-particle space are 17, 11, 33, 19, and 31, respectively.

The introduction of collective coordinates is an important subject in the study of nuclear collective motions. For large-amplitude collective motions, it is crucial to construct optimal collective coordinates self-consistently [52]. As for the an-harmonic quadrupole vibrations of nuclei with relatively low excitation energies, it was shown that, if noncollective couplings are included faithfully, the dependence on the selection of the collective coordinates becomes small, and stable results are obtained [33]. In this work, as a choice of the collective coordinates, the so-called adiabatic TD mode [33] is adopted. Possibilities of different choices of the representation were investigated in Ref. [33], and it was shown that the noncollective couplings play crucial roles to stabilize the results of numerical calculations and to remove the sensitive dependence on the particular choice of the collective coordinates.

Then, by use of the BET, the original fermion Hamiltonian is mapped to the corresponding boson Hamiltonian and is expanded up to fourth order with respect to the collective boson. Effects of the noncollective branches are included by use of the Feschbach formalism [53] with the closure approximation for the intermediate states in the coupling Hamiltonian [5]. For the collective branch, to include the RPA-type correlations at the early stage of the calculation [5], a transformation from the A bosons to the so-called α bosons is introduced as $A^\dagger = \psi \alpha^\dagger + \phi \tilde{\alpha}$, $\tilde{A} = \phi \alpha^\dagger + \psi \tilde{\alpha}$ with $\psi^2 - \phi^2 = 1$. Since the present formalism is based on the quasiparticle representation, the approximate number projection method [32] is carried out to remove the spurious proton- and neutron-pairing rotational modes.

The resultant collective Hamiltonian is diagonalized in the collective subspace of the boson Hilbert space to obtain energy spectra as well as boson wave functions for low-lying collective states. The basis vectors of the collective subspace are expressed as $|\mathcal{N} v \eta I M)$, where $\mathcal{N}$ is the boson number, v is the seniority number, I is the spin with its projection M, and η is an additional quantum number necessary for a complete labeling of the basis vectors.

III. RESULTS AND DISCUSSION

A. Boson description of Os isotopes around $N = 116$

Prior to discussing details of the individual ^{192}Os, to see characteristics of the microscopic BET description of osmium isotopes around $N = 116$, an overview is presented here for the evolution of contents of the collective bosons and that of the shape of collective potentials due to changes in the number of neutrons.

In Fig. 1, two-quasiparticle probabilities in the adiabatic collective TD mode calculated for ^{192}Os are illustrated and compared with those for ^{190,194}Os [38]. For ^{192}Os, 10 major components contained in the collective TD mode are $\pi(h_{11/2})^2$, $\pi(d_{3/2}, s_{1/2})$, $\nu(h_{9/2}, f_{5/2})$, $\nu(f_{5/2})^2$, $\nu(i_{13/2})^2$, $\nu(p_{3/2})^2$, $\nu(p_{3/2}, p_{1/2})$, $\pi(d_{5/2}, s_{1/2})$, $\pi(d_{3/2})^2$, and $\nu(i_{13/2}, g_{9/2})$ in descending order, and their total occupancy is 71.7%, while for ^{190}Os, they are $\nu(i_{13/2})^2$, $\nu(h_{9/2}, f_{5/2})$, $\pi(h_{11/2})^2$, $\pi(d_{3/2}, s_{1/2})$, $\nu(p_{3/2})^2$, $\pi(d_{5/2}, s_{1/2})$, $\nu(f_{7/2}, p_{3/2})$, $\pi(d_{3/2})^2$, $\nu(i_{13/2}, g_{9/2})$, and $\nu(f_{5/2})^2$, and their total occupancy is 74.1%, and for ^{194}Os, they are $\nu(f_{5/2})^2$, $\pi(h_{11/2})^2$, $\nu(f_{5/2}, p_{1/2})$, $\nu(p_{3/2}, p_{1/2})$, $\pi(d_{3/2}, s_{1/2})$, $\nu(h_{9/2}, f_{5/2})$, $\pi(d_{5/2}, s_{1/2})$, $\nu(p_{3/2})^2$, $\nu(i_{13/2}, g_{9/2})$, and $\pi(d_{3/2})^2$, and their total occupancy becomes 74.7%. From Fig. 1, one can see that the change in the composition of the major components of the collective TD mode due to the change in the number of neutrons is relatively small for protons but is conspicuous for neutrons, which reflects properties of quasiparticle states around Fermi levels. Since the collective TD mode is a primal building block of the collective boson mode in the present formalism, the evolution of the basic TD mode as the number of neutrons changes is closely related to the change in the structure of the collective boson, which is essential for the boson description of nuclear structures.

In Fig. 2, the theoretical potential-energy surfaces calculated by means of the BET are presented for ^{190,192,194}Os [38]. The potential of ^{192}Os has a minimum point on the prolate side ($\beta_{\min}^P = 0.175$, $V_{\min}^P = -3.014$ MeV) and a saddle point on the oblate side ($\beta_{\text{sad}}^O = -0.175$, $V_{\text{sad}}^O = -2.992$ MeV). The difference in energy on both sides, $V^{PO} = V_{\text{sad}}^O - V_{\min}^P$, is 0.022 MeV: the absolute value of it is rather small compared to the energy of the zero-point oscillation, 0.96 MeV, evaluated relative to the absolute minimum of the potential. This feature of the potential implies strong softness or instability for the γ deformation. Compared with ^{192}Os, the potential of ^{190}Os is slightly prolate favored, while that of ^{194}Os tends to be oblate favored. The evolution of the BET potential with changes in the number of neutrons suggests a prolate-oblate shape transition at around $N = 116$ for osmium isotopes [38], which is compatible with the predictions of Refs. [9–12].

In the calculations of Robledo *et al.* [10] using the self-consistent Hartree-Fock-Bogoliubov (HFB) approximation with Gogny D1S and Skyrme SLy4 interactions, when passing through the γ degrees of freedom, there appear minimums in the potentials for osmium isotopes around $N = 116$, though
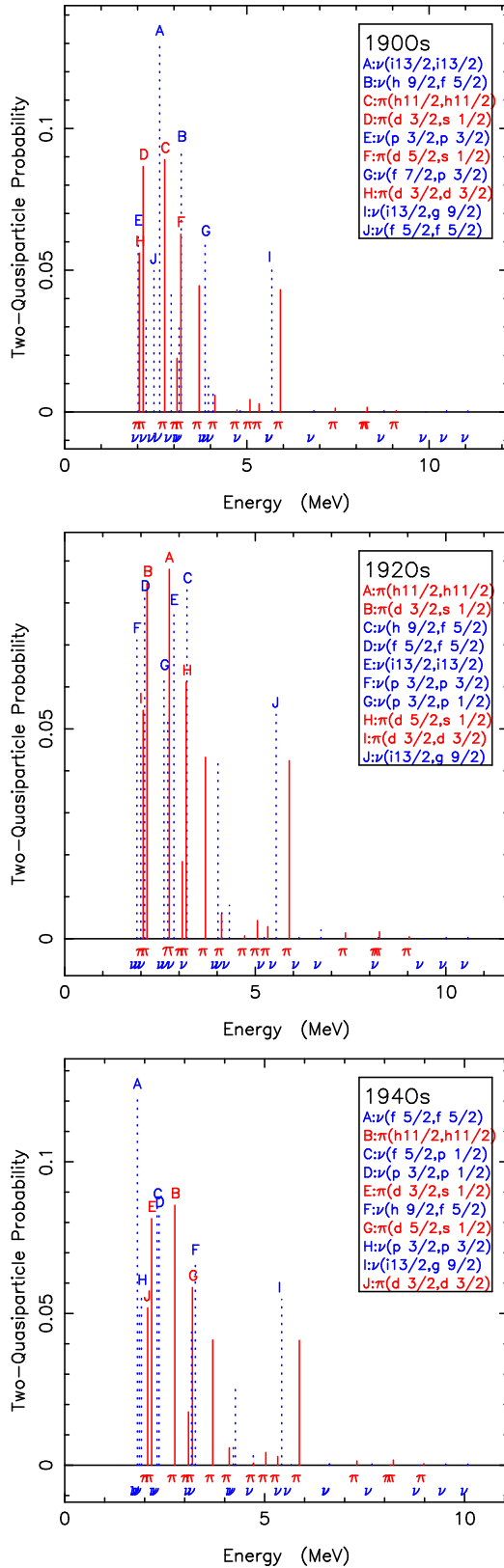
FIG. 1. Two-quasiparticle probabilities in the adiabatic collective TD mode for ^{190,192,194}Os are plotted against the two-quasiparticle energies. The scripts π and ν are attached to distinguish the proton components (solid red lines) and the neutron components (dotted blue lines). Figure adapted from Ref. [38].
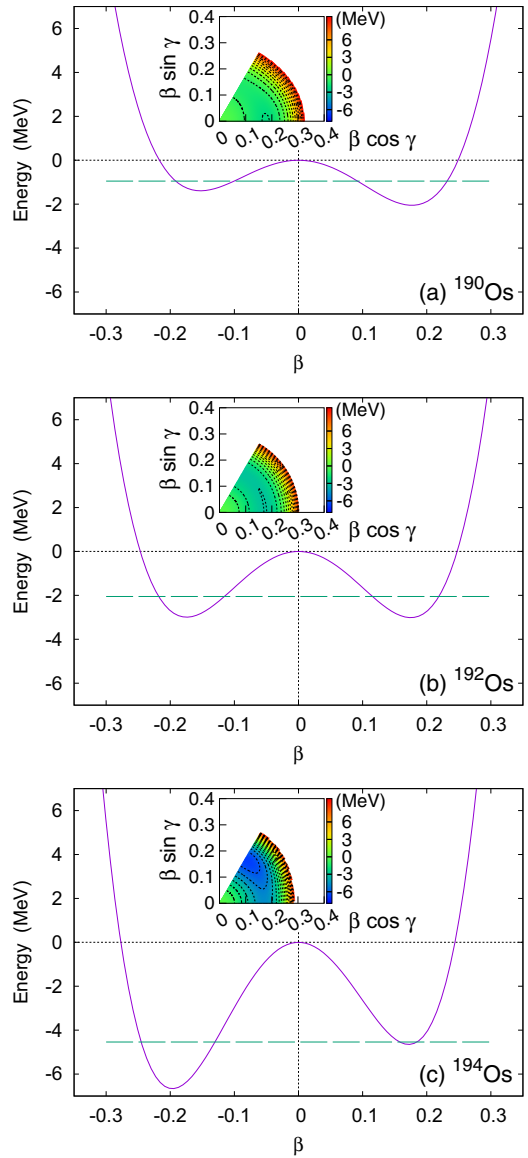
FIG. 2. Evolution of collective potentials as the number of neutrons changes around $N = 116$. Theoretical potential energy surfaces are plotted as a function of quadrupole deformation β for (a) ^{190}Os, (b) ^{192}Os, and (c) ^{194}Os. The horizontal dashed lines indicate the ground-state energies. The inserted figures are contour maps of the potentials drawn in steps of 1 MeV. The interaction strengths chosen to fit spectrums are $(f, g') = (1.04, 1.05)$, $(1.15, 1.05)$, and $(1.35, 1.00)$ for ^{190}Os, ^{192}Os, and ^{194}Os, respectively [38].

the minimums are in all the cases very shallow and never reach a depth of more than 0.5 MeV below the axially symmetric saddle points. On the other hand, in the present work, since the microscopic Hamiltonian is expanded up to the fourth order in terms of the collective bosons, the γ dependence of the potential is limited only up to the order of $\beta^3 \cos 3\gamma$ and the potential varies monotonically with γ. To improve the γ dependence of the potentials in the present type of analysis, further investigations based on a much higher order boson expansion are advisable [35]. As for the interacting boson model (IBM), it has been pointed out that only the inclusion of
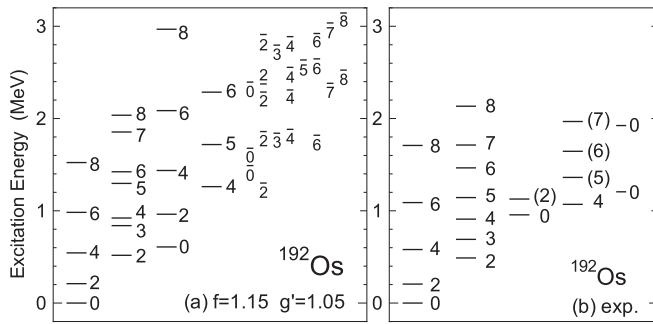
FIG. 3. (a) Theoretical energy levels for ^{192}Os. The states in the ground band, the quasi-γ band, the $0_2{}^+$ band, and the $K = 4$ band are separately accumulated, while other states (short bars) are assembled in their spin groups in columnar forms. (b) The experimental spectrum for ^{192}Os. Beside the major four bands adopted in Ref. [59], the 0_3^+ and 0_4^+ states identified in Ref. [60] are shown by short bars in the last column. Figure adapted from Ref. [38].

higher order terms, e.g., three-body *boson* interactions, in the Hamiltonian can lead to triaxial equilibrium shapes [54–58]. A detailed description on the use of higher order terms in the IBM and on its connection with the existence of double-γ phonon states in ^{166}Er have been reported in Refs. [56,57].

B. Boson wave functions of ^{192}Os

In Fig. 3, theoretical energy levels for ^{192}Os calculated in this work are illustrated and compared with experimental levels. The energies of the ground-state band and those of the quasi-γ band are qualitatively reproduced, though the staggering of the quasi-γ band is too prominent in the theory. For the 0_2^+ band, the energy of the bandhead state in the theoretical spectrum seems too low compared to that of the *possible* $K = 0$ band listed in Ref. [59]. The calculated intervals of the energy levels for the 0_2^+ band and those for the $K = 4$ band appear to be too wide compared to the experimental data, though the identifications of the excited members of these bands are tentative in Ref. [59]. Further details on the level structure and electromagnetic properties of ^{192}Os are discussed in the next subsection, and in the rest of this subsection, for later discussion, major components of the boson wave functions for some relevant states of ^{192}Os are described.

In the present numerical calculations, states with $\mathcal{N} \leqslant 18$ are taken, which amount to a diagonalization space of slightly less than 100-dimensional matrices for each spin I. Figure 4 illustrates the probability distributions of the boson numbers $\mathcal{N}$ and the seniorities v in the theoretical wave functions for 0_1^+, 0_2^+, 0_3^+, and 0_4^+ states, and similar illustrations are presented in Fig. 5 for 2_1^+, 2_2^+, 2_3^+, and 2_4^+ states and in Fig. 6 for 4_1^+, 4_2^+, 4_3^+, and 4_4^+ states. From these figures, one can verify the selection rules for the possible values of v [61] are satisfied and can also see to what degree the boson wave functions converge in terms of v and $\mathcal{N}$ in the present numerical calculations.

In the boson wave functions of ^{192}Os, the leading-order component of the ground state is $|\mathcal{N}, v) = |0, 0)$ followed by
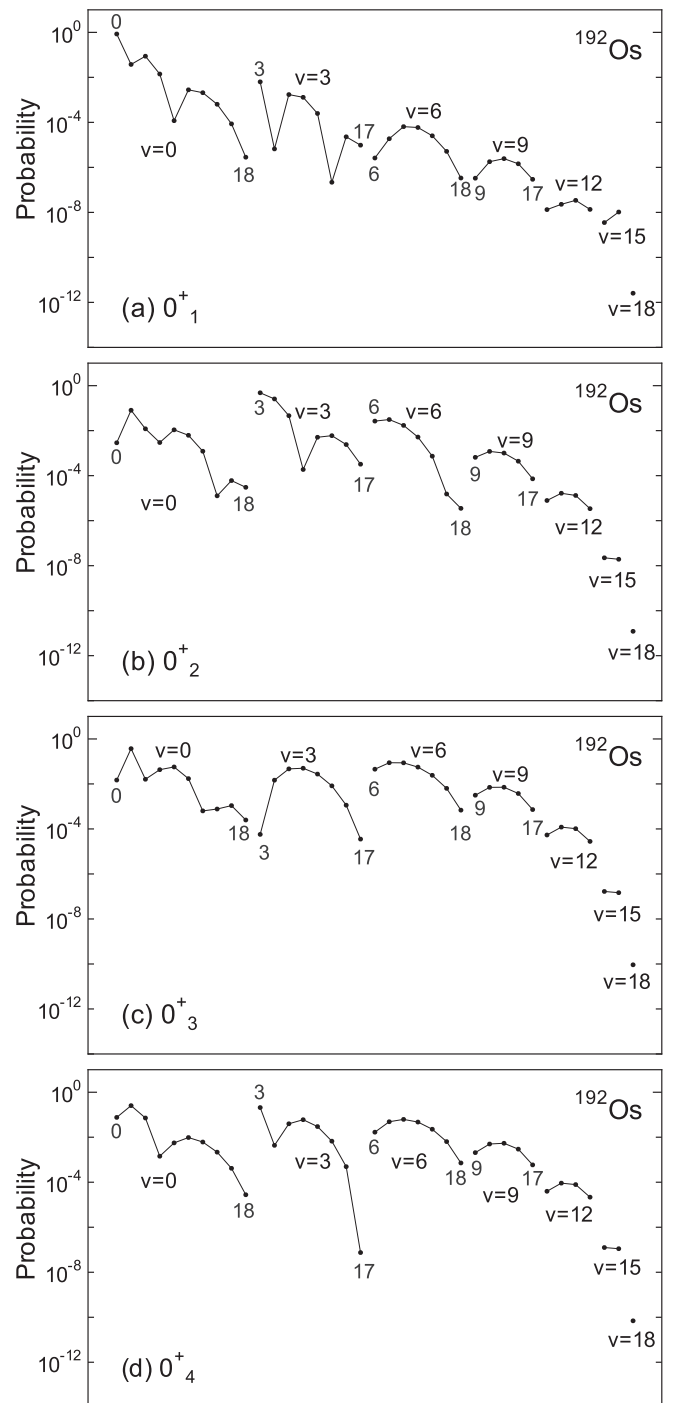
FIG. 4. Probability distributions of the boson numbers $\mathcal{N}$ and the seniorities v in the theoretical wave functions for $0_1{}^+$, $0_2{}^+$, $0_3{}^+$, and $0_4{}^+$ states in ^{192}Os. Components of the same seniority are separately accumulated and connected in the ascending order of $\mathcal{N}$. The numbers attached at some beginning or ending points represent the boson numbers. Figure for $0_1{}^+$ is adapted from Ref. [38].

$|4, 0)$, $|2, 0)$, and so forth. For the lowest four 0^+ states shown in Fig. 4, the major $|\mathcal{N}, v)$ components of each boson wave function are written in descending order, up to at least four

terms and the total probability exceeds 70%, as

$$|0_1^+) = 0.920|0,0) - 0.295|4,0) + 0.194|2,0) + 0.119|6,0),$$
$$|0_2^+) = 0.694|3,3) - 0.507|5,3) - 0.284|2,0) + 0.215|7,3),$$
$$|0_3^+) = 0.609|2,0) - 0.296|8,6) + 0.295|10,6) + 0.239|8,0) - 0.237|12,6) - 0.224|9,3),$$
$$|0_4^+) = -0.505|2,0) - 0.457|3,3) + 0.276|0,0) + 0.268|4,0) + 0.250|10,6) - 0.246|9,3). \tag{14}$$

In the same way, the major $|\mathcal{N}, v)$ components of each boson wave function for the lowest four 2^+ states shown in Fig. 5 are written as

$$|2_1^+) = -0.896|1,1) + 0.259|2,2) + 0.174|5,1) - 0.168|7,1),$$
$$|2_2^+) = -0.833|2,2) + 0.364|4,2) - 0.292|1,1) - 0.152|5,5),$$
$$|2_3^+) = 0.531|4,4) - 0.518|6,4) + 0.344|8,4) - 0.259|3,1),$$
$$|2_4^+) = 0.469|7,5) - 0.407|9,5) - 0.383|5,5) + 0.279|11,5) + 0.241|2,2) + 0.205|8,2), \tag{15}$$

those for the lowest four 4^+ states shown in Fig. 6 are written as

$$|4_1^+) = -0.813|2,2) + 0.350|4,2) + 0.282|3,3) - 0.225|5,3),$$
$$|4_2^+) = 0.682|3,3) - 0.447|5,3) + 0.332|2,2) - 0.190|4,2),$$
$$|4_3^+) = 0.603|4,4) - 0.540|6,4) + 0.328|8,4) - 0.202|3,3),$$
$$|4_4^+) = -0.463|7,5) + 0.391|9,5) + 0.388|5,5) - 0.261|11,5) - 0.231|2,2)$$
$$- 0.186|8,2) + 0.151|12,8) - 0.150|10,8), \tag{16}$$

and, in addition, those for the 3_1^+ and 5_1^+ states are written as

$$|3_1^+) = 0.760|3,3) - 0.528|5,3) + 0.217|7,3) - 0.178|8,6),$$
$$|5_1^+) = 0.624|4,4) - 0.563|6,4) + 0.346|8,4) - 0.173|9,7). \tag{17}$$

The above equations seem to manifest the general tendency that the higher the excitation energy of a state, the more the boson wave function of that state is dispersed in many $|\mathcal{N}, v)$ components. It is interesting to find possible origins of the major components of the wave functions in some cases of Eqs. (14)–(17) in connection with the schematic illustration of the relationship between the vibrational and rotational models proposed by Sakai [62].

C. Level structure and electromagnetic properties

In Tables I and II, electromagnetic properties of ^{192}Os predicted by the present BET for the case of $e_{\text{pol}}(E2) = 0.5e$ are summarized and compared with experimental data together with predictions of some available theories, namely, the adiabatic time-dependent Hartree-Bogolyubov (ATDHB) method studied by Kumar and Baranger [3], the general collective model (GCM) studied by Hess *et al.* [8], the sextic and Mathieu approach (SMA) studied by Raduta and Buganu [39], the quasiparticle-phonon model (QPM) studied by Iudice and Sushkov [40], and the IBM mapped from the Gogny-D1S studied by Nomura *et al.* [11].

Considering that there are only three fitting parameters, f, g', and $e_{\text{pol}}(E2)$, the present calculations seem to reproduce the overall patterns of the spectrum and the electromagnetic properties almost reasonably, though there are some points that have not been reached in detail as discussed below.

1. The ground-state band

For the states in the ground-state band, as can be seen in Fig. 3 and Table I, the present calculations reproduce experiments well for both the excitation energies and the intraband $E2$ transitions. Concerning the quadrupole moments, as shown in Table II, the BET predicts a value close to the experiments of the 2_1^+ state, but overestimates the experimental moments of the 4_1^+, 6_1^+, and 8_1^+ states.

2. The quasi-γ band

The excitation energies of the states in the quasi-γ band are qualitatively reproduced, though the staggering of the band is too prominent in the theory (Fig. 3).

Experimental $B(E2; I \to I - 2)$ values for intraband transitions in the quasi-γ band have been reported for transitions between even-spin states [59]. For these intraband transitions, as shown in Table I, current BET tends to overestimate the $B(E2)$ values, though each theoretical value has the same order as the corresponding experiment.

So far, experimental values of quadrupole moments in the quasi-γ band are only available for even-spin states: Their signs are positive for the bandhead state and negative for the 4_2^+, 6_2^+, and 8_2^+ states. In the BET results for the quadrupole moments, the experimental value is reproduced well for the bandhead state, while for the 4_2^+ state the theoretical value has an opposite sign compared to the experiment, and for the 6_2^+ and 8_2^+ states, though the theory reproduces the signs of
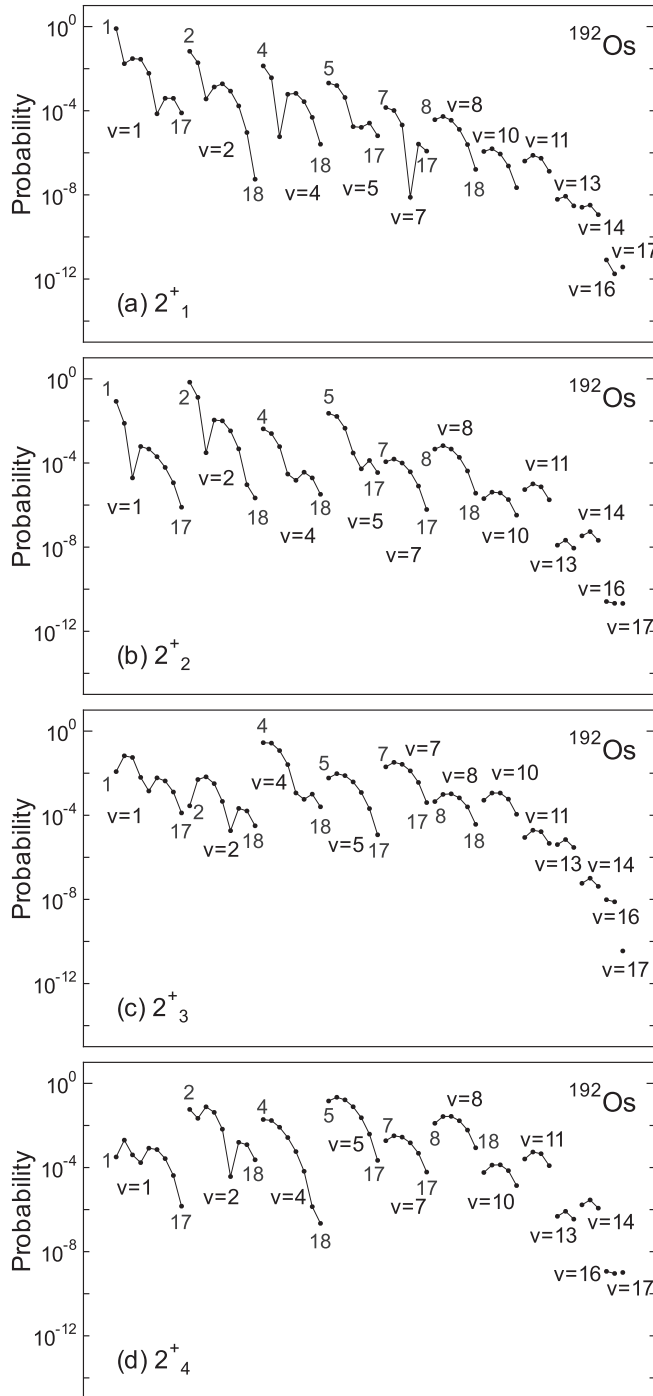
FIG. 5. The same as in Fig. 4 but for $2_1{}^+$, $2_2{}^+$, $2_3{}^+$, and $2_4{}^+$ states in ^{192}Os. Figure for $2_1{}^+$ is adapted from Ref. [38].

FIG. 6. The same as in Fig. 4 but for $4_1{}^+$, $4_2{}^+$, $4_3{}^+$, and $4_4{}^+$ states in ^{192}Os.

the experiments, the absolute values of the moments are considerably underestimated. The present calculations seem to reproduce roughly the tendency that the sign of the quadrupole moments in the quasi-γ band in ^{192}Os changes from positive to negative as the spin increases.

In terms of the α-boson representation, as one sees in Eq. (15), the main component of the wave function of the $2_2{}^+$ state is $|2_2^+\rangle \approx |2, 2\rangle \approx [\alpha^\dagger \alpha^\dagger]^{(2)}|0\rangle \approx \gamma^\dagger|0\rangle$, where

$|0\rangle$ is the α-boson vacuum, and for later use $\gamma^\dagger$ is introduced very naively as a symbolic representation of the operator that creates an excitation of the γ mode. Then, from Eqs. (16) and (17) the main component of the $4_2{}^+$ state and that of the $3_1{}^+$ state are expressed very naively as $|4_2^+\rangle \approx |3, 3\rangle^{(I=4)} \approx [\alpha^\dagger \gamma^\dagger]^{(4)}|0\rangle$ and $|3_1^+\rangle \approx |3, 3\rangle^{(I=3)} \approx [\alpha^\dagger \gamma^\dagger]^{(3)}|0\rangle$, respectively. It is also interesting to see in Eqs. (15)–(17) that there are very rough relationships of

TABLE I. Electromagnetic properties of ^{192}Os. The values given are $B(E2; I_i \rightarrow I_f)$ in units of $(eb)^2$. For comparison, predictions of the adiabatic time-dependent Hartree-Bogolyubov (ATDHB) method studied by Kumar and Baranger [3], the general collective model (GCM) studied by Hess *et al.* [8], the sextic and Mathieu approach (SMA) studied by Raduta and Buganu [39], the quasiparticle-phonon model (QPM) studied by Iudice and Sushkov [40], and the IBM mapped from the Gogny-D1S studied by Nomura *et al.* [11] are listed. Experimental data are taken from Ref. [59].

Transition	I_i	I_f	BET	ATDHB	GCM	SMA	QPM	IBM(D1S)[a]	Expt.[b]
g → g	2_1	0_1	0.415	0.515	0.674	0.424		0.409	0.409(4)
	4_1	2_1	0.610	0.781	0.913	0.632		0.563	0.497(13)
	6_1	4_1	0.711		1.077	0.858			$0.658(^{+35}_{-21})$
	8_1	6_1	0.779		1.188	1.030			0.757(38)
$\gamma \rightarrow \gamma$	3_1	2_2	0.448	0.736					
	4_2	2_2	0.420		0.334	0.261			$0.298(^{+9}_{-12})$
	4_2	3_1	0.120						
	5_1	3_1	0.407						
	5_1	4_2	0.158						
	6_2	4_2	0.608		0.502	0.352			$0.339(^{+21}_{-42})$
	6_2	5_1	0.0910						
	7_1	5_1	0.580						
	7_1	6_2	0.0731						
	8_2	6_2	0.736			0.549			$0.314(^{+46}_{-38})$
	8_2	7_1	0.063						
$0_2^+ \rightarrow 0_2^+$	2_3	0_2	0.283	0.468					
	4_4	2_3	0.418						
	6_4	4_4	0.543						
$4_3^+ \rightarrow 4_3^+$	5_2	4_3	0.509						
	6_5	5_2	0.585						
$\gamma \rightarrow g$	2_2	0_1	0.0680	0.007	0.0098	0.006	0.0393	0.0011	0.037(1)
	2_2	2_1	0.482	0.743	0.679	0.303		0.56	$0.303(^{+17}_{-8})$
	2_2	4_1	0.0001	0.000		0.000			$0.024(^{+28}_{-5})$
	3_1	2_1	0.113	0.013					
	3_1	4_1	0.167	0.297					
	4_2	2_1	0.0397		0.031	0.004			0.0019(2)
	4_2	4_1	0.297		0.346	0.068			$0.203(^{+24}_{-12})$
	4_2	6_1	0.8×10^{-4}			0.000			$0.017(^{+9}_{-10})$
	6_2	4_1	0.0342			0.002			
	6_2	6_1	0.230			0.042			$0.171(^{+36}_{-14})$
$0_2^+ \rightarrow g$	0_2	2_1	0.0599	0.0082			0.0106		$0.0040(^{+11}_{-12})$
	2_3	0_1	0.0078	0.0014					
	2_3	2_1	0.0028	0.000					
	2_3	4_1	0.0361	0.044					
$0_2^+ \rightarrow \gamma$	0_2	2_2	0.825	0.714	0.303		0.0743	0.63	0.20(2)
	2_3	2_2	0.3×10^{-4}	0.010					0.0025(3)
	2_3	3_1	0.397	0.282					0.0141(14)
	2_3	4_2	0.122						
	4_4	2_2	0.0057						
$4_3^+ \rightarrow \gamma$	4_3	2_2	0.095				0.0554		$0.069(^{+6}_{-10})$
	4_3	3_1	0.382						$0.296(^{+39}_{-78})$
	4_3	4_2	0.319						$0.157(^{+22}_{-27})$
$4_3^+ \rightarrow g$	4_3	2_1	0.0022						$0.0014(^{+14}_{-7})$
$4_3^+ \rightarrow 0_2^+$	4_3	2_3	0.0174						
Others	0_3	2_1	0.0518						0.0016(6)
	0_3	2_2	0.0455						
	0_3	2_3	0.0744						
	0_4	2_1	0.0232						
	0_4	2_2	0.104						
	0_4	2_3	0.0166						
	4_5	2_2	0.0058						
	6_3	5_2	0.0311						
	6_4	5_2	0.0164						

[a]Values are normalized to the experimental $B(E2; 2_1^+ \rightarrow 0_1^+)$ value.
[b]Values in parentheses represent uncertainties in the least significant digits.

$|4_2^+\rangle \approx \alpha^\dagger |2_2^+\rangle$ and $|5_1^+\rangle \approx \alpha^\dagger |3_1^+\rangle$ in the present calculations for ^{192}Os.

3. The 0_2^+ band and the excited 0^+ states

Concerning the 0_2^+ band, as already mentioned, the energy of the bandhead in the theoretical spectrum seems too low and the calculated intervals of the energy levels appear to be too wide compared to the *possible K = 0* band listed in Ref. [59].

In the pioneering works by Kumar and Baranger [3], by applying the ATDHB method, the seven functions of the Bohr's collective Hamiltonian were derived for the P+Q model of residual interactions, and by solving numerically the collective Hamiltonian it was predicted that the 0_2^+ states of osmium nuclei near $A = 190$ are predominantly three phonon stats.

In the present results, one can see in Fig. 4 and Eq. (14) that the main contribution to the boson wave function of the 0_2^+ state comes from the three-phonon component, which is compatible with the prediction by Kumar and Baranger [3], and the two-phonon component is rather dominant in the 0_3^+ and 0_4^+ states.

In Tables I and III, one sees for the levels of the 0_2^+ band that $E2$ transition strengths to the ground-state band tend to be rather small compared to those to the quasi-γ band, which implies that it is difficult to interpret the 0_2^+ state as a typical β vibrational state. For the calculated $E2$ transitions, this property can be understood as follows [36]: In terms of the α-boson representation, as one sees in Eq. (14), the main component of the wave function of the 0_2^+ state of ^{192}Os is expressed as $|0_2^+\rangle \approx (\alpha^\dagger \alpha^\dagger \alpha^\dagger)|0\rangle \approx (\alpha^\dagger \cdot \gamma^\dagger)|0\rangle$, where $(\alpha^\dagger \alpha^\dagger \alpha^\dagger) \equiv (\alpha^\dagger \cdot [\alpha^\dagger \alpha^\dagger]^{(2)})$, while, as already mentioned, that of the 2_2^+ state is $|2_2^+\rangle \approx [\alpha^\dagger \alpha^\dagger]^{(2)}|0\rangle \approx \gamma^\dagger|0\rangle$. Since the leading order term of the $E2$ transition operator in the BET is $T(E2) \approx (\alpha^\dagger + \alpha)$, the transition from the 0_2^+ state to the 2_2^+ state becomes strong.

In the wave function of the 0_2^+ state, one finds a considerable amount of such a component of a collective α-boson excitation build on the 2_2^+ state. In Ref. [69], Casten and von Brentano proposed the interpretation that the lowest $K = 0$ intrinsic excitation of deformed nuclei is not a β vibration but rather a collective phonon built on the γ vibration, though it is not clear whether this excitation should be viewed as an *independent K = 2* excitation superposed on the γ band or as a two-phonon double γ vibration. Although ^{192}Os is a transitional nucleus and for deformed nuclei it must be fair to investigate the precision of the proposal elsewhere separately, in the present numerical results there seems to be a possibility that the 0_2^+ state of ^{192}Os possesses similarity to the state discussed in Ref. [69]. The properties of the calculated 0_2^+ state mentioned above for the case of ^{192}Os appear to be similar to those for the case of ^{128}Ba [36]. One of the reasons may be seen in the similarity between the collective potential of ^{192}Os shown in Fig. 2 and that of ^{128}Ba reported in Ref. [36]: Both potentials have two axial minimums of approximately equal depth, indicating considerable γ softness, though the collective potential of ^{192}Os is shallower than that of ^{128}Ba in the BET calculations.

Regarding the excited 0^+ states of ^{192}Os, three levels, namely 0_2^+(956 keV), 0_3^+(1206 keV), and 0_4^+(1924 keV),

TABLE II. Quadrupole moments of ^{192}Os. The values given are $Q(I^\pi)$ in units of eb. For comparison, predictions of the ATDHB method studied by Kumar and Baranger [3] and the GCM studied by Hess *et al.* [8] are listed. The last column shows references for experimental data.

I^π	BET	ATDHB	GCM	Expt. [a]	Ref.
2_1^+	-0.7678	-0.359	-0.937	$-0.96(3)$	[63]
				$-0.80(18)$	[64]
				$-0.86(20)$	[65]
				$-0.917(^{+45}_{-129})$	[13]
4_1^+	-1.019	-0.408		$-0.550(^{+196}_{-45})$	[13]
6_1^+	-1.163			$-0.809(^{+77}_{-181})$	[13]
8_1^+	-1.218			$-0.844(^{+116}_{-232})$	[13]
2_2^+	0.7963	0.340	0.916[b]	$0.8(3)$[c]	[66]
				$0.747(^{+34}_{-64})$	[13]
4_2^+	0.2720			$-0.626(^{+68}_{-60})$	[13]
6_2^+	-0.0281			$-0.941(^{+77}_{-258})$	[13]
8_2^+	-0.0818			$-0.586(^{+316}_{-219})$	[13]
2_3^+	-0.5195	-0.570	-1.470 [b]		
2_4^+	0.4965				
4_3^+	0.5494			$0.965(^{+113}_{-309})$	[13]
4_4^+	-0.4986				

[a]Values in parentheses represent uncertainties in the least significant digits.

[b]The ambiguous correspondence between these two values and the two 2^+ states due to a misprint in Table 2 of Ref. [8] is fixed here by estimation [67].

[c]In Refs. [59,68], this experimental value is cited in reverse sign, which seems to be a typographic error resolving the sign problem stated in Ref. [38].

have been identified by the (t, p) reaction studied by Flynn and Burke [60]. The first three rows of Table III compare branching ratios

$$R(0_n^+) \equiv \frac{B(E2; 0_n^+ \to 2_2^+)}{B(E2; 0_n^+ \to 2_1^+)} \tag{18}$$

for $n = 2, 3$, and 4. Unfortunately, for these ratios so far, experimental values are only available in the 0_2^+ state, and theoretical ratios available are rather limited. For the ratio $R(0_2^+)$, BET and QPM underestimate while ATDHB overestimates the experiment. As one sees in Table I, BET overestimates both $B(E2; 0_2^+ \to 2_2^+)$ and $B(E2; 0_2^+ \to 2_1^+)$, QPM underestimates the former and overestimates the latter, while ATDHB overestimates both of them. However, in all of these theories and the experiment, the 0_2^+ state of ^{192}Os decays much more strongly to the 2_2^+ state than to the 2_1^+ state, which probably indicates that the 0_2^+ state contains a certain amount of the γ-phonon component as already discussed in terms of the boson wave functions. In the present results of BET, among the 0_2^+, 0_3^+, and 0_4^+ states, the 0_2^+ state has the largest ratio $R(0_n^+)$. For the excitation energy ratio $E(0_2^+)/E(2_2^+)$, the experimental value is about 1.96, which suggests that the 0_2^+ state may be a candidate for a two-phonon

TABLE III. $B(E2)$ ratios in ^{192}Os. For comparison, predictions of the ATDHB method studied by Kumar and Baranger [3], the GCM studied by Hess *et al.* [8], the SMA studied by Raduta and Buganu [39], the QPM studied by Iudice and Sushkov [40], and the IBM mapped from the Gogny-D1S studied by Nomura *et al.* [11] are listed. Experimental data are taken from Ref. [59].

I_i	I_f	BET	ATDHB	GCM	SMA	QPM	IBM(D1S)	Expt.[a]
0_2	$2_2/2_1$	13.8	87.			7.0		53.(17)
0_3	$2_2/2_1$	0.879						
0_4	$2_2/2_1$	4.49						
2_2	$0_1/2_1$	0.141	0.009	0.014	0.02		0.002	0.12(1)
3_1	$2_1/2_2$	0.252	0.018					
3_1	$4_1/2_2$	0.373	0.379					
4_2	$4_1/2_2$	0.707		1.09	0.26			0.68(11)
4_3	$2_1/2_2$	0.0232						0.020(23)
4_3	$2_2/3_1$	0.249						0.233(96)
4_3	$4_2/3_1$	0.835						0.53(23)
5_1	$4_2/3_1$	0.388						
6_2	$6_1/4_2$	0.378			0.12			0.50(17)

[a]Values in parentheses represent uncertainties in the least significant digits.

double γ ($0_{\gamma\gamma}{}^+$) excitation, while in the present BET too small value of the energy ratio, i.e., 1.18, is a remaining issue.

In addition, in the present BET analyses for ^{192}Os, a certain amount of β vibrational components may be dispersed in the $0_2{}^+$, $0_3{}^+$, and $0_4{}^+$ states. In fact, as one sees in Eq. (14), the $0_2{}^+$ wave function contains a small but not negligible amount of $|2, 0\rangle$ component while in both the $0_3{}^+$ and $0_4{}^+$ wave functions $|2, 0\rangle$ is the major component, and calculated $E2$ transitions from these states to the $2_1{}^+$ state are significant (about 9.1, 7.9, and 3.5 W.u. for $0_2{}^+$, $0_3{}^+$, and $0_4{}^+$, respectively), though such large $E2$ transitions have not yet been observed experimentally.

For the $0_4{}^+$ state, present BET calculation shows a significant $E2$ transition to the $2_2{}^+$ state, which may indicate that the $0_4{}^+$ state contains a certain amount of the double-γ component, though such transitions have not yet been observed experimentally.

Regarding the 0_2^+ states in deformed nuclei, various discussions [15,69–71] have been made against the conventional interpretation that those are the β vibrations [45]. The low-lying 0^+ states probably posses rather complex characteristics. The nature of the 0^+ states requires extensive investigations, including analyses of two-nucleon transfer strengths, which provide more precise identification of components of the wave functions in terms of the β vibrational mode, pairing vibrations, multiphonon excitations based on the γ vibration, among others.

4. The $K^\pi = 4^+$ band

There have been various discussions about the nature of the $K^\pi = 4^+$ bands in Os isotopes [13,17–20,40,72–74]. As for the $K^\pi = 4^+$ band of ^{192}Os listed in Ref. [59], the spin assignments of the members are tentative except for the bandhead state and intraband $B(E2)$ values have not yet been determined experimentally.

In the present BET, from the theoretical $B(E2)$ of Table I, candidates corresponding to the first three members of the band are considered to be 4_3^+, 5_2^+, and 6_5^+ states. In terms of the α boson representation, as one sees in Eq. (16), the main

component of the 4_3^+ state is very naively expressed as $|4_3^+\rangle \approx |4, 4\rangle \approx [[\alpha^\dagger\alpha^\dagger]^{(2)}[\alpha^\dagger\alpha^\dagger]^{(2)}]^{(4)}|0\rangle \approx [\gamma^\dagger\gamma^\dagger]^{(4)}|0\rangle$. Thus one may expect that the 4_3^+ state contains the two-phonon $\gamma\gamma$ component with a sizable amplitude.

For the 4_3^+ state, the $B(E2)$ intensity ratio

$$R_{4/2}^T \equiv \frac{B(E2; 4_3^+ \to 2_2^+)}{B(E2; 2_2^+ \to 0_1^+)} \qquad (19)$$

is of interest to compute. Among the theories mentioned in Table I, the $B(E2)$ values required to obtain $R_{4/2}^T$ are available for BET and QPM [40], and Table IV compares those theoretical values with the experiments. From the standpoint of considering the 4_3^+ state as the double-γ structure, the experimental $R_{4/2}^T$ of ^{192}Os seems to be close to the harmonic limit, i.e., 2, while both theoretical ratios are much smaller than the limit, showing significant anharmonicities. For the energy ratio $R_{4/2}^E \equiv E(4_3^+)/E(2_2^+)$, the current BET value is shown in Table V and compared with the experimental ratio together with the QPM prediction. Both the experimental ratio and the QPM prediction are close to the harmonic limit, while the BET value is about 10% larger than the experiment.

It is reported in Ref. [40] that the $K^\pi = 4^+$ QPM state contains the two-phonon $\gamma\gamma$ component with a sizable amplitude, but the one-phonon hexadecapole component is larger, accounting for about 67% of the QPM wave function for ^{192}Os.

As mentioned in Sec. II B, in the present framework of BET, all the TD elements with spin $I \leqslant 4$ constructed in

TABLE IV. $B(E2)$ values of transitions $2_2^+ \to 0_1^+$ and $4_3^+ \to 2_2^+$ in units of W.u., and their ratio for ^{192}Os. For comparison, results of the QPM studied by Iudice and Sushkov [40] are listed. Experimental data are taken from Ref. [75].

	BET	QPM	Expt.
$B(E2; 2_2^+ \to 0_1^+)$	10.3	5.98	5.6 ± 0.2
$B(E2; 4_3^+ \to 2_2^+)$	14.4	8.42	$11. \pm 1$
$R_{4/2}^T$	1.40	1.42	1.87 ± 0.25

TABLE V. Excitation energies of 2_2^+ and 4_3^+ states in units of MeV, and their ratio for ^{192}Os. For comparison, results of the QPM studied by Iudice and Sushkov [40] are listed. Experimental data are taken from Ref. [75].

	BET	QPM	Expt.
$E(2_2^+)$	0.518	0.423	0.489
$E(4_3^+)$	1.26	0.913	1.070
$R_{4/2}^E$	2.44	2.16	2.19

the Fermion model space are regarded as the chosen modes. Among the chosen modes the lowest quadrupole mode is identified as the collective mode, and effects of all the other chosen (noncollective) modes, except for the spurious (pairing rotational) modes, are included perturbatively. Hence, the effects of hexadecapole modes are included in the present calculations through the noncollective couplings. However, that is a prescription allowed when all the relevant hexadecapole modes are not very collective. Possibilities of the emergence of strong hexadecapole modes may need to be investigated, where the inclusion of the self-consistent hexadecapole interaction [41] into the Fermion Hamiltonian is called for to evaluate faithfully the collectiveness of hexadecapole modes. When collective hexadecapole modes emerge, some nonperturbative treatments of those modes may be required for better descriptions of the $K^\pi = 4^+$ band, which will be discussed elsewhere in the future.

IV. SUMMARY AND CONCLUSIONS

Low-lying collective states of ^{192}Os are studied by means of the BET with the self-consistent effective interactions. The evolution of the building blocks of the collective boson and that of the potentials due to changes in the number of neutrons are examined for ^{190,192,194}Os to confirm characteristics of the microscopic boson description of osmium isotopes near $N = 116$ [38]. The evolution of the BET potentials suggests a prolate-oblate shape transition at around $N = 116$ for osmium isotopes, which is compatible with the predictions of Refs. [9–12]. The theoretical potential of ^{192}Os has two axial minima, one on the prolate side and the other on the oblate side, with rather small difference in depth compared to the energy of the zero-point oscillation, which implies strong softness or instability for the γ deformation.

For some relevant states of ^{192}Os, the structures of the boson wave functions are illustrated, showing the degree of convergence of the present BET calculations. With the help of the structural analysis of the boson wave functions, properties of some low-lying states and relevant quasibands are discussed.

The theoretical level energies and electromagnetic properties of ^{192}Os are compared to experimental data. The excitation energies of the ground-state band and the quasi-γ band are qualitatively reproduced, though the staggering of the quasi-γ band is too prominent in the theory. The theoretical intervals of the energy levels for the 0_2^+ band and those for the $K = 4$ band appear to be too wide compared to the experimental data [59]. For the 0_2^+ band, the energy of the bandhead state in the theoretical spectrum seems too low compared to that of the *possible* $K = 0$ band listed in Ref. [59].

In the present calculations, the main contribution to the boson wave function of the 0_2^+ state of ^{192}Os comes from the three-phonon component, and the two-phonon component is rather dominant in the 0_3^+ and 0_4^+ states.

Although some points that have not been reached in detail need to be improved in the future, considering that there are only three fitting parameters, f, g', and $e_{\text{pol}}(E2)$, and as a result all of these values are close to their respective standard values, the present BET description of collective states in ^{192}Os seems to be promising.

[1] A. Faessler, W. Greiner, and R. K. Sheline, Phys. Rev. **135**, B591 (1964).

[2] K. Kumar and M. Baranger, Phys. Rev. Lett. **17**, 1146 (1966).

[3] K. Kumar and M. Baranger, Nucl. Phys. A **110**, 529 (1968); **122**, 273 (1968).

[4] T. Kishimoto and T. Tamura, Nucl. Phys. A **192**, 246 (1972).

[5] T. Kishimoto and T. Tamura, Nucl. Phys. A **270**, 317 (1976).

[6] K. J. Weeks and T. Tamura, Phys. Rev. C **22**, 1323 (1980).

[7] R. F. Casten and J. A. Cizewski, Nucl. Phys. A **309**, 477 (1978); **425**, 653 (1984).

[8] P. O. Hess, J. Maruhn, and W. Greiner, J. Phys. G **7**, 737 (1981).

[9] P. Sarriguren, R. Rodriguez-Guzman, and L. M. Robledo, Phys. Rev. C **77**, 064322 (2008).

[10] L. M. Robledo, R. Rodriguez-Guzman, and P. Sarriguren, J. Phys. G **36**, 115104 (2009).

[11] K. Nomura, T. Otsuka, R. Rodriguez-Guzman, L. M. Robledo, P. Sarriguren, P. H. Regan, P. D. Stevenson, and Z. Podolyak, Phys. Rev. C **83**, 054303 (2011).

[12] N. Al-Dahan, P. H. Regan, Z. Podolyak, P. M. Walker, N. Alkhomashi, G. D. Dracoulis, G. Farrelly, J. Benlliure, S. B. Pietri, R. F. Casten *et al.*, Phys. Rev. C **85**, 034301 (2012).

[13] C. Y. Wu, D. Cline, T. Czosnyka, A. Backlin, C. Baktash, R. M. Diamond, G. D. Dracoulis, L. Hasselgren, H. Kluge, B. Kotlinski *et al.*, Nucl. Phys. A **607**, 178 (1996).

[14] J. M. Allmond, R. Zaballa, A. M. Oros-Peusquens, W. D. Kulp, and J. L. Wood, Phys. Rev. C **78**, 014302 (2008).

[15] J. F. Sharpey-Schafer, The Structure of Excited 0^+ States in Nuclei and the Effect of the γ Degree of Freedom, in *Proceedings of the International Conference on Frontiers in Nuclear*

Structure, Astrophysics, and Reactions, Rhodes, Greece, 2010, edited by P. Demetriou, R. Julin, and S. Harissopulos, AIP Conf. Proc. No. 1377 (AIP, New York, 2011), p. 205.

[16] M. R. Macphail, R. F. Casten, and W. R. Kane, Phys. Lett. **59**, 435 (1975).

[17] C. Y. Wu and D. Cline, Phys. Lett. B **382**, 214 (1996).

[18] C. Y. Wu, D. Cline, A. B. Hayes, M. W. Simon, R. Krucken, J. R. Cooper, C. J. Barton, C. W. Beausang, C. Bialik, M. A. Caprio *et al.*, Phys. Rev. C **64**, 014307 (2001).

[19] C. Y. Wu, D. Cline, A. B. Hayes, M. W. Simon, R. Krücken, J. R. Cooper, C. J. Barton, C. W. Beausang, C. Bialik, M. A. Caprio *et al.*, Phys. Rev. C **66**, 039802 (2002).

[20] D. G. Burke, Phys. Rev. C **66**, 039801 (2002).

[21] T. Kishimoto and T. Tamura, Phys. Rev. C **27**, 341 (1983).

[22] A. Klein and E. R. Marshalek, Rev. Mod. Phys. **63**, 375 (1991).

[23] B. Sørensen, Nucl. Phys. A **97**, 1 (1967); **119**, 65 (1968); **142**, 392 (1970).

[24] S. G. Lie and G. Holzwarth, Phys. Rev. C **12**, 1035 (1975).

[25] T. Tamura, K. J. Weeks, and T. Kishimoto, Phys. Rev. C **20**, 307 (1979).

[26] K. J. Weeks and T. Tamura, Phys. Rev. C **22**, 888 (1980).

[27] T. Tamura, K. J. Weeks, and T. Kishimoto, Nucl. Phys. A **347**, 359 (1980).

[28] A. Bohr, B. R. Mottelson, and D. Pines, Phys. Rev. **110**, 936 (1958).

[29] S. T. Belyaev, Mat. Fys. Medd. Dan. Vid. Selsk. **31**, 11 (1959).

[30] L. S. Kisslinger and R. A. Sorensen, Mat. Fys. Medd. Dan. Vid. Selsk. **32**, 9 (1960).

[31] L. S. Kisslinger and R. A. Sorensen, Rev. Mod. Phys. **35**, 853 (1963).

[32] H. Sakamoto and T. Kishimoto, Nucl. Phys. A **486**, 1 (1988).

[33] H. Sakamoto and T. Kishimoto, Nucl. Phys. A **528**, 73 (1991).

[34] H. Sakamoto, Phys. Rev. C **52**, 177 (1995).

[35] H. Sakamoto, Phys. Rev. C **64**, 024303 (2001).

[36] H. Sakamoto, Phys. Rev. C **93**, 034315 (2016).

[37] H. Sakamoto, Acta Phys. Pol. B **48**, 573 (2017).

[38] H. Sakamoto, J. Phys.: Conf. Ser. **1555**, 012023 (2020).

[39] A. A. Raduta and P. Buganu, Phys. Rev. C **83**, 034313 (2011).

[40] N. Lo Iudice and A. V. Sushkov, Phys. Rev. C **78**, 054304 (2008).

[41] H. Sakamoto and T. Kishimoto, Nucl. Phys. A **501**, 205 (1989); **501**, 242 (1989).

[42] H. Sakamoto, J. Phys.: Conf. Ser. **1023**, 012003 (2018).

[43] S. G. Nilsson, C. F. Tsang, A. Sobiczewski, Z. Szymański, S. Wycech, C. Gustafson, I.-L. Lamm, P. Möller, and B. Nilsson, Nucl. Phys. A **131**, 1 (1969).

[44] B. R. Mottelson, *Nikko Summer School Lectures* (NORDITA, Copenhagen, 1967), Vol. 288.

[45] A. Bohr and B. R. Mottelson, *Nuclear Structure* (Benjamin, New York, 1975), Vol. 2.

[46] T. Kishimoto, J. M. Moss, D. H. Youngblood, J. D. Bronson, C. M. Rozsa, D. R. Brown, and A. D. Bacher, Phys. Rev. Lett. **35**, 552 (1975).

[47] T. Kishimoto, Giant resonances in deformed nuclei, in *Proceedings of the International Conference on Highly Excited States in Nuclear Reaction* (RCNP, Osaka, 1980), p. 145; Higher-

order-coupling Hamiltonian induced by self-consistency, in *Proceedings of the International Conference on Highly Excited States in Nuclear Reaction* (RCNP, Osaka, 1980), p. 377.

[48] T. Kishimoto, T. Tamura, and T. Kammuri, Prog. Theor. Phys. Suppl. **74–75**, 170 (1983).

[49] E. R. Marshalek, Phys. Rev. Lett. **51**, 1534 (1983); Phys. Rev. C **29**, 640 (1984); Phys. Lett. **244**, 1 (1990).

[50] J. Copnell, K. Kumar, S. J. Robinson, and C. Tenreito, J. Phys. G **18**, 1943 (1992).

[51] H. Sakamoto and T. Kishimoto, Phys. Lett. **245**, 321 (1990).

[52] T. Marumori, T. Maskawa, F. Sakata, and A. Kuriyama, Prog. Theor. Phys. **64**, 1294 (1980).

[53] H. Feshbach, Ann. Phys. **5**, 357 (1958); **19**, 287 (1962).

[54] P. Van Isacker and J.-Q. Chen, Phys. Rev. C **24**, 684 (1981).

[55] K. Heyde, P. Van Isacker, M. Waroquier, and J. Moreau, Phys. Rev. C **29**, 1420 (1984).

[56] J. E. García-Ramos, C. E. Alonso, J. M. Arias, and P. Van Isacker, Phys. Rev. C **61**, 047305 (2000).

[57] J. E. García-Ramos, J. M. Arias, and P. Van Isacker, Phys. Rev. C **62**, 064309 (2000).

[58] K. Nomura, N. Shimizu, D. Vretenar, T. Nikšić, and T. Otsuka, Phys. Rev. Lett. **108**, 132501 (2012).

[59] C. M. Baglin, Nucl. Data Sheets **113**, 1871 (2012).

[60] E. R. Flynn and D. G. Burke, Phys. Rev. C **17**, 501 (1978).

[61] E. Chacón, M. Moshinsky, and R. T. Sharp, J. Math. Phys. **17**, 668 (1976).

[62] M. Sakai, Nucl. Phys. A **104**, 301 (1967).

[63] M. V. Hoehn, E. B. Shera, H. D. Wohlfahrt, Y. Yamazaki, R. M. Steffen, and R. K. Sheline, Phys. Rev. C **24**, 1667 (1981).

[64] C. Y. Chen, J. X. Saladin, and A. A. Hussein, Phys. Rev. C **28**, 1570 (1983).

[65] C. S. Lim, R. H. Spear, W. J. Vermeer, M. P. Fewell, and G. J. Gyapong, Nucl. Phys. A **485**, 399 (1988).

[66] C. Baktash, J. X. Saladin, J. J. O'Brien, and J. G. Alessi, Phys. Rev. C **22**, 2383 (1980).

[67] P. O. Hess (private communication).

[68] P. Raghavan, At. Data Nucl. Data Tables **42**, 189 (1989).

[69] R. F. Casten and P. von Brentano, Phys. Rev. C **50**, R1280 (1994).

[70] P. E. Garrett, J. Phys. G: Nucl. Part. Phys. **27**, R1 (2001).

[71] F.-Q. Chen and J. L. Egido, Phys. Rev. C **93**, 064313 (2016).

[72] M. Oshima, T. Morikawa, H. Kusakari, N. Kobayashi, M. Sugawara, Y. H. Zhang, A. Ferragut, S. Ichikawa, N. Shinohara, Y. Nagame, M. Shibata, Y. Gono, and T. Inamura *et al.*, Nucl. Phys. A **557**, 635 (1993).

[73] A. A. Phillips, P. E. Garrett, N. Lo Iudice, A. V. Sushkov, L. Bettermann, N. Braun, D. G. Burke, G. A. Demand, T. Faestermann, P. Finlay *et al.*, Phys. Rev. C **82**, 034321 (2010).

[74] J. F. Sharpey-Schafer, No low-lying nuclear vibrations: Configuration dependent pairing and axial asymmetry, in *Proceedings of the 54th International Conference on Winter Meeting on Nuclear Physics* (PoS, SISSA, Bormio, Italy, 2016).

[75] ENSDF data base http://www.nndc.bnl.gov.